

Kondo lattice behavior in the ordered dilute magnetic semiconductor $\text{Yb}_{14-x}\text{La}_x\text{MnSb}_{11}$ B. C. Sales,¹ P. Khalifah,^{1,2} T. P. Enck,¹ E. J. Nagler,¹ R. E. Sykora,^{3,4} R. Jin,¹ and D. Mandrus¹¹Condensed Matter Sciences Division, Oak Ridge National Laboratory, Oak Ridge, Tennessee 37831, USA²Chemistry Department, University of Massachusetts, Amherst, Massachusetts 01003, USA³Chemical Sciences Division, Oak Ridge National Laboratory, Oak Ridge, Tennessee 37831, USA⁴Chemistry Department, University of South Alabama, Mobile, Alabama 36688-0002, USA

(Received 4 August 2005; published 30 November 2005)

We report Hall, magnetic, heat capacity, and doping studies from single crystals of $\text{Yb}_{14}\text{MnSb}_{11}$ and $\text{Yb}_{13.3}\text{La}_{0.7}\text{MnSb}_{11}$. These heavily doped semiconducting compounds are ferromagnetic below 53 and 39 K, respectively. The renormalization of the carrier mass from $2m_e$ near room temperature to $20m_e$ at 5 K, plus the magnetic evidence for partial screening of the Mn magnetic moments suggest that these compounds represent rare examples of an underscreened Kondo lattice with $T_K \approx 285$ K.

DOI: [10.1103/PhysRevB.72.205207](https://doi.org/10.1103/PhysRevB.72.205207)

PACS number(s): 75.50.Pp, 75.30.Mb, 72.15.Qm, 75.50.Cc

Ferromagnetic semiconductors are envisioned as a key component of many proposed spintronic devices that functionalize both the electron charge and spin.^{1,2} There have been many theories of the origin of ferromagnetism in doped semiconductors,³ but it has been difficult to obtain a clean comparison between theory and experiment because of problems associated with clustering or phase separation of magnetic dopants in the semiconducting host. In the present paper we show that it is productive to investigate the ferromagnetism in stoichiometric compounds such as $\text{Yb}_{14}\text{MnSb}_{11}$ ($T_c=53$ K). In this heavily doped semiconducting compound the magnetic Mn atoms are at a unique crystallographic site in the structure resulting in a minimum Mn-Mn separation of 10 Å. Using a combination of Hall, heat capacity, magnetic data, and doping studies we are able to show that the ferromagnetism is likely mediated by relatively heavy quasiparticles that form due to the Kondo interaction. This leads to the nonintuitive and surprising result that using carrier tuning to increase T_c can result in a reduced saturation moment. Since the local environment of each Mn atom is similar to that found in the heavily studied III-V semiconductors⁴ (such as GaAs:Mn), the present results may also have significant implications for III-V materials as well.

To the best of our knowledge the compound $\text{Yb}_{14}\text{MnSb}_{11}$ was first synthesized by Chan *et al.* in 1998.⁵ It is isostructural with a large family of related Zintl compounds such as $\text{Ca}_{14}\text{AlSb}_{11}$ and $\text{Ca}_{14}\text{MnSb}_{11}$ (Ref. 6) crystallizing with a tetragonal lattice in the space group $I41/acd$. The structure of $\text{Yb}_{14}\text{MnSb}_{11}$ is shown in Fig. 1, where for clarity only the Mn and four nearest neighbor Sb atoms are shown. Previous magnetization and x-ray magnetic circular dichroism (XMCD) measurements indicate that Yb is divalent in this compound with no magnetic moment.^{5,7} Initial magnetization and magnetic susceptibility measurements suggested a Mn^{+3} (d^4) configuration.^{5,8} The MnSb_4 tetrahedron is somewhat distorted with angles of 105.6° and 117.5° which were previously interpreted as a Jahn-Teller distortion associated with a d^4 configuration.⁵ However, more recent XMCD measurements are more consistent with a Mn^{+2} (d^5) configuration with the moment of one spin compensated by the anti-

aligned spin of an Sb 5p hole from the Sb_4 cage surrounding the Mn.⁷ There is also a substantial distortion of the AlSb_4 tetrahedra in the isostructural compound $\text{Ca}_{14}\text{AlSb}_{11}$ implying that steric effects cause distortions even in the absence of Jahn-Teller effects.⁹ A d^5+h picture is also expected from detailed electronic structure calculations on related $\text{Ca}_{14}\text{MnBi}_{11}$ compounds.¹⁰ This is in accord with the understanding of the most heavily studied dilute magnetic semiconductor (DMS) GaAs:Mn which is suggested by multiple experiments to have also a d^5+h Mn configuration.^{2,3,11}

We grew relatively large (up to 0.5 g) single crystals of $\text{Yb}_{14}\text{MnSb}_{11}$ with and without various dopants (La, Te, Y, Sc, etc.) capable of modifying the carrier concentration using the

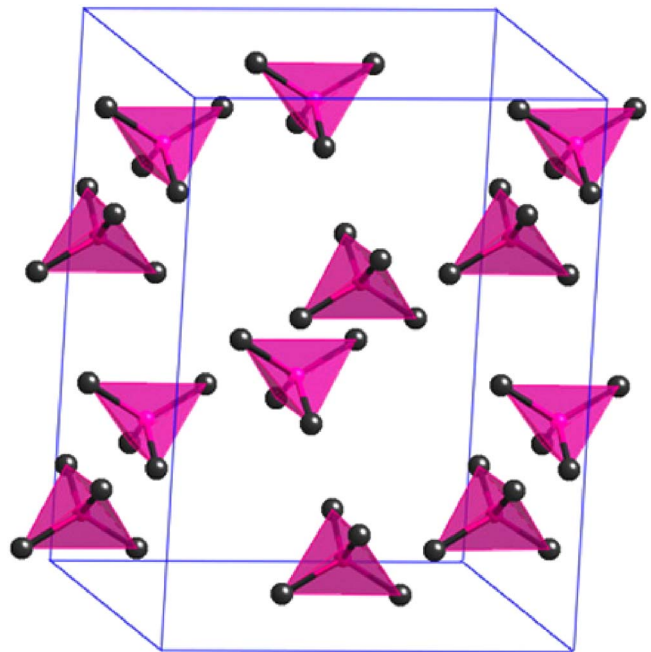


FIG. 1. (Color online) Structure of the tetragonal compound $\text{Yb}_{14}\text{MnSb}_{11}$ with $a=16.61$ Å and $c=21.95$ Å. For clarity only the Mn atoms and the nearest neighbor Sb atoms (black) are shown. The closest Mn-Mn distance is 9.98 Å.

conditions worked out by Fisher *et al.*⁸ for pure $\text{Yb}_{14}\text{MnSb}_{11}$. From a variety of different doping experiments, we concluded that the maximum amount of Yb that could be replaced by La, Y, or Sc was 5%, 4.5%, and 4%, respectively. At these doping levels, the T_c of the crystals were 39 ± 1 , 38 ± 1 , and 37 ± 1 K, respectively. The partial substitution of La for Yb resulted in the largest crystals and hence of the doped samples we investigated these crystals in the most detail. A single crystal structure refinement of a La-doped crystal (Bruker SMART APEX CCD x-ray diffractometer) indicates a composition of $\text{Yb}_{13.3}\text{La}_{0.7}\text{MnSb}_{11}$ with all of the La atoms substituting on an Yb site [$a=16.6613(6)$ Å, $c=21.9894(7)$ Å]. This is expected since La^{+3} and Yb^{+2} ions are about the same size and are chemically similar. Hall effect, resistivity, and heat capacity data were obtained using a physical property measurement system from quantum design on oriented and thinned single crystals. Hall and resistivity data were obtained using a standard six lead method and either rotating the sample by 180° in a fixed magnetic field or by sweeping the direction of the field from positive to negative values. The Hall data were qualitatively the same regardless of the orientation of the crystal with respect to the current or field directions. Magnetization data were obtained using a commercial superconducting quantum interference device magnetometer from quantum design.

Heat capacity data from both materials are shown in Fig. 2. The transitions to the ferromagnetic phases are evident at $T_c=53$ K ($\text{Yb}_{14}\text{MnSb}_{11}$ crystal) and $T_c=39$ K ($\text{Yb}_{13.3}\text{La}_{0.7}\text{MnSb}_{11}$ crystal). The small concentration of magnetic Mn atoms, and the relatively large lattice contribution to the heat capacity data near T_c make it difficult to accurately determine the magnetic contribution to the heat capacity data below T_c . The electronic contribution to the heat capacity, γT , can be reliably estimated, however, by using the heat capacity data from the lowest temperatures ($T \leq 5$ K) and plotting C/T vs T^2 . This analysis yields $\gamma \sim 58$ mJ/K² mole Mn for the La-doped crystal and $\gamma \sim 160$ mJ/K² mole Mn for the undoped crystal. The value of γ for the undoped crystal is very similar to the values previously measured by Fisher *et al.*⁸ and Burch *et al.*¹² However, to determine the significance of γ requires a measure of the carrier concentration and an estimate of the expected band mass.

The carrier concentrations for the crystals are determined from a detailed analysis of Hall data that takes into account the anomalous Hall effect (AHE) associated with the ferromagnetism. For many ferromagnets it has been experimentally demonstrated¹³ that the Hall resistivity $\rho_{xy} = R_0 B + R_s M$, where R_0 is the normal Hall coefficient, B is the magnetic field, M is the magnetization, and R_s is the anomalous Hall coefficient. In the simplest situations R_0 is proportional to $1/n$, where n is the effective carrier concentration. There are a variety of theories and models for the AHE, which can be viewed as an additional current that develops in the y direction in response to an electric field in the x direction (magnetization in z direction).^{14–16} There can be both intrinsic ($\rho_{xy} \propto \rho_{xx}^2$) and extrinsic contributions ($\rho_{xy} \propto \rho_{xx}$) to the AHE that are usually separated based on how ρ_{xy} depends on the normal resistivity ρ_{xx} .¹³ Interest in spin currents for spin based electronics, coupled with new theoretical insights into

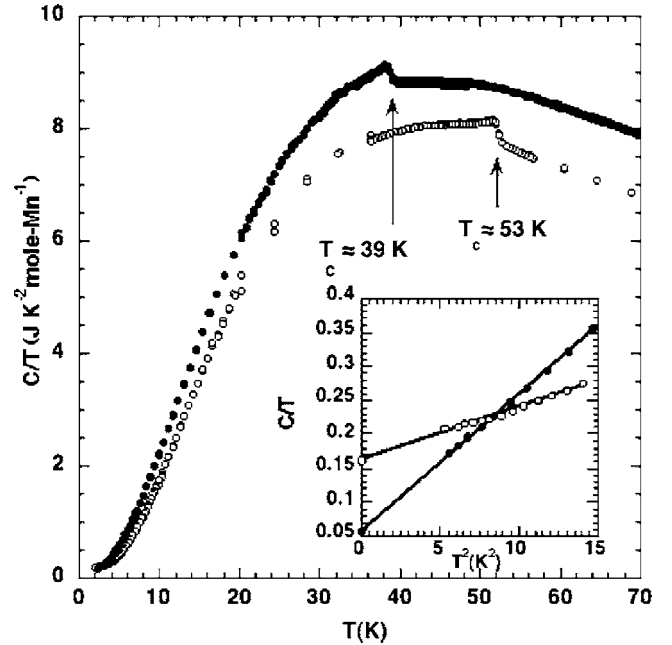


FIG. 2. Heat capacity divided by temperature (C/T) vs temperature (T) for single crystals of $\text{Yb}_{14}\text{MnSb}_{11}$ and $\text{Yb}_{13.3}\text{La}_{0.7}\text{MnSb}_{11}$. The ferromagnetic phase transition for each crystal is noted. Analysis of these data at low temperatures (inset) yields values for the electronic heat coefficient of $\gamma=160 \pm 10$ mJ/K² mole Mn, and $\gamma = 58 \pm 5$ mJ/K² mole Mn for the undoped and La-doped crystals, respectively. Heat capacity data on both crystals were taken down to 0.5 K and in magnetic fields up to 14 T (not shown). The data were corrected for a small nuclear Schottky contribution that was significant for temperatures below 1 K.

the microscopic origin of R_s , have stimulated substantial recent interest in the AHE. While the AHE of $\text{Yb}_{14}\text{MnSb}_{11}$ and related alloys are quite interesting, these data will be discussed in more detail in a future publication. The measured Hall resistivity for $\text{Yb}_{14}\text{MnSb}_{11}$ is shown in Fig. 3. Analysis of these data (as described in the figure caption) indicates that the carrier concentration is about 1.0×10^{21} to 1.35×10^{21} holes/cm³ above T_c , depending on how the data are analyzed, but increasing to 1.9×10^{21} holes/cm³ for temperatures well below T_c . All of the measured carrier concentrations are typical of a heavily doped semiconductor and the values correspond to approximately 1 hole/Mn (1 hole per Mn gives 1.3×10^{21} holes/cm³). Doping the crystals with a small amount of La (i.e., $\text{Yb}_{13.3}\text{La}_{0.7}\text{MnSb}_{11}$) lowers the measured hole concentration to about 4×10^{20} holes/cm³ (see Fig. 4). This observation is consistent with the simple idea that the extra electrons contributed to the compound when part of the Yb^{+2} ions are replaced by La^{+3} ions fill some of the holes in the Sb $5p$ bands. A crude estimate for the band gap of ~ 1 eV is obtained from the optical data of Burch *et al.*¹² on $\text{Yb}_{14}\text{MnSb}_{11}$, but it is not clear if the carrier concentration in these materials can be reduced enough to observe a gap with electrical transport measurements.

The average Fermi wave vector k_F only depends on the number of carriers per unit volume and is given by $k_F = (3\pi^2 n)^{1/3} \sim 0.36$ Å⁻¹. The Fermi energy E_F from the free electron model is given by $\hbar^2 k_F^2 / (4\pi^2 m_e)$, which gives E_F

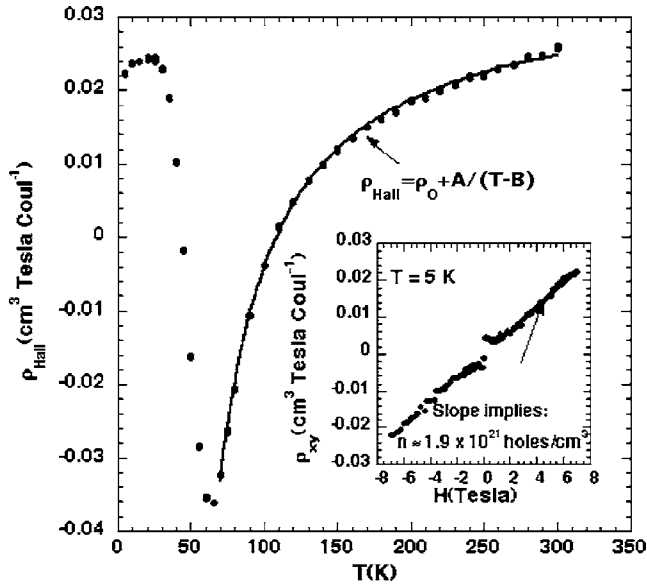


FIG. 3. Hall resistivity (ρ_{xy}) vs. temperature for $\text{Yb}_{14}\text{MnSb}_{11}$ measured in a field of 7 T. The carrier concentration is estimated by fitting the data above $T_c \sim 53$ K to a constant plus a Curie-Weiss Law. Similar data (not shown) were also taken with a field of 1 T. This analysis yields an average value for the carrier concentration above T_c of 1.35×10^{21} holes/cm³. Comparable values for the carrier concentration are obtained if the measured magnetization data are used. If the Hall resistivity above T_c is analyzed using the expression derived for Kondo lattice compounds above the coherence temperature (Ref. 22) (the anomalous part of the Hall resistivity $R_S M$ is replaced by $C \rho_{xy} M$, where C is a constant), the data yield a temperature independent ($75 \text{ K} \leq T \leq 300 \text{ K}$) carrier concentration of $1.03 \pm 0.05 \times 10^{21}$ holes/cm³. The carrier concentration well below T_c is estimated by plotting ρ_{xy}/B vs M/B using the measured magnetization data as shown in the inset. This analysis yields a carrier concentration of 1.9×10^{21} holes/cm³. It appears that from just above T_c ($T \approx 75 \text{ K}$) to well below T_c , the carrier concentration jumps by about 0.9×10^{21} holes cm⁻³.

$=0.5$ eV. If the band mass $m_b \approx 1.8m_e$, is used (as measured from optical data¹² or estimated from electronic structure calculations,¹⁰ or estimated¹⁷ from the room temperature Seebeck coefficient of $+44 \mu\text{V/K}$) $E_F \sim 0.28$ eV. The measured values for the carrier concentration indicate a substantial mass enhancement for the carriers of about $20m_e$ for the undoped crystal and $11m_e$ for the La-doped crystal. These mass enhancement values suggest a Kondo energy scale of $0.5 \text{ eV}/20 = 0.025 \text{ eV}$ or $T_K \sim 285 \text{ K}$ for the undoped crystal, and $T_K \sim 210 \text{ K}$ for the doped crystal. Similar mass enhancement values and estimates of the Kondo temperature were obtained by Burch *et al.*¹² for the undoped crystal using optical and heat capacity data. In addition, Burch *et al.*¹² were able to map the evolution of the enhanced carrier mass as both the temperature and frequency were lowered toward zero. They also noted that the optical data were qualitatively similar to that found in many Kondo lattice compounds.

The basic Kondo interaction describes the antiferromagnetic interaction between a localized spin (in this case a Mn d^5 configuration) and the mobile carriers, which for $\text{Yb}_{14}\text{MnSb}_{11}$ would be $5p$ holes from the Sb bands. A material with a regular array of these spins (or Kondo centers) is

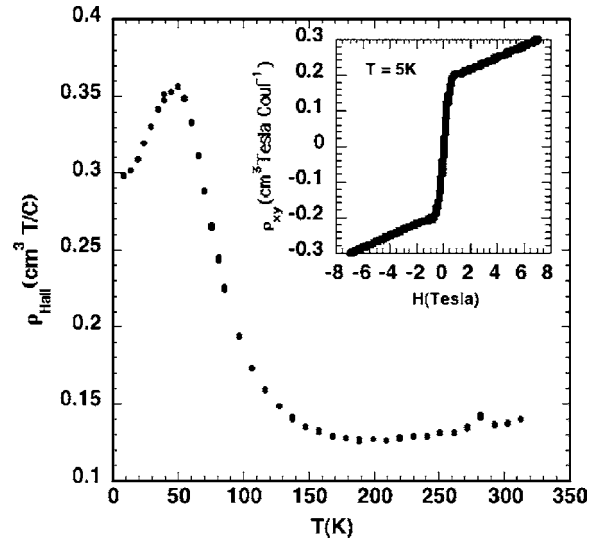


FIG. 4. Hall resistivity versus temperature for $\text{Yb}_{13.3}\text{La}_{0.7}\text{MnSb}_{11}$ single crystals. An analysis of these data indicates a carrier concentration of 4×10^{20} holes cm⁻³.

referred to as a Kondo lattice compound. While the Kondo interaction is often associated with the formation of a non-magnetic singlet and a large enhancement of the carrier mass, this same interaction is also responsible for Ruderman-Kittel-Kasuya-Yoshida (carrier mediated exchange) coupling between spins which can result in magnetic order.¹⁸ In rare cases, such as CePdSb , both effects can occur which results in ferromagnetic order but with a reduced saturation moment.¹⁹ Dietl *et al.*¹¹ have shown that in Mn-doped III-V semiconductors there is a strong tendency for the Kondo interaction to bind holes from the neighboring group Vp bands to the d shell of the Mn⁺² impurity resulting in a composite object with a net magnetic moment of $4\mu_B$. The binding energy of the holes in $\text{Yb}_{14}\text{MnSb}_{11}$ is relatively weak and is roughly given by $T_K \approx 285 \text{ K}$. The standard estimate for the size of the Kondo compensation cloud is $h\nu_F/2\pi k_B T_K \approx 30 \text{ \AA}$, which also indicates weak binding. At temperatures near T_K the composite quasiparticles should begin to break up with less compensation of the Mn d^5 moments by the $5p$ holes.

The magnetic data from the undoped and doped crystals are consistent with this picture. The replacement of Yb by La reduces the number of carriers and weakens the indirect exchange coupling, resulting in a lower T_c . The lower number of holes also reduces the magnetic screening of the Mn d^5 moments, which results in a larger saturation magnetic moment, as is observed (see Fig. 5). In addition, a careful analysis of the magnetic susceptibility data of $\text{Yb}_{14}\text{MnSb}_{11}$ above T_c indicates an increase in the effective moment for temperatures near $T_K \sim 285 \text{ K}$ as the composite quasiparticles break up (see Fig. 6). A similar effect should also be observed for the doped crystal. However, because of the reduced screening, the effective moment below T_K is too close to the unscreened value expected above T_K so that within experimental error no effect is measurable. Our work suggests that the unusual d^5+h magnetism of Mn atoms may be intrinsic to many dilute magnetic semiconductors. This leads to the non-

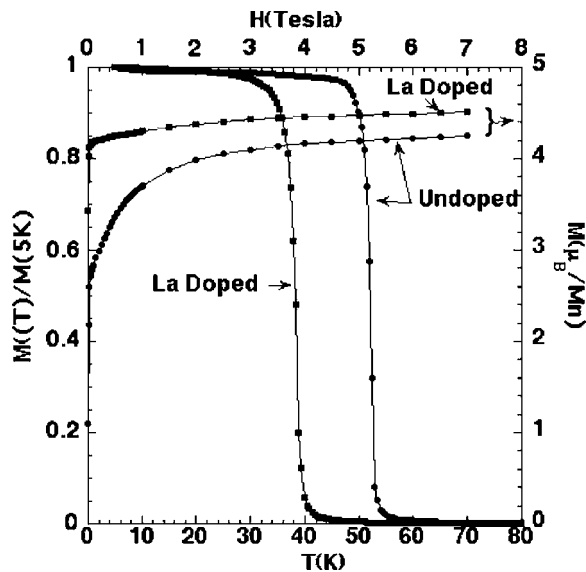


FIG. 5. Normalized magnetization (left scale) vs temperature for crystals cooled in a field of 100 Oe. The Curie temperature of the $\text{Yb}_{14}\text{MnSb}_{11}$ crystal is $T_c = 53 \pm 1$ K, a value consistent with values previously reported (Refs. 5 and 8). Magnetization (right scale) vs applied magnetic field for $\text{Yb}_{14}\text{MnSb}_{11}$ and $\text{Yb}_{13.3}\text{La}_{0.7}\text{MnSb}_{11}$ single crystals. Although the T_c of the La-doped crystal is lower, the saturation magnetization is about $4.5\mu_B$ per Mn as compared to about $4.2\mu_B$ per Mn for the undoped crystals.

intuitive and surprising result that using carrier tuning to increase T_c can result in a reduced saturation moment. The present data also support the idea, proposed by Burch *et al.*,¹² that $\text{Yb}_{14}\text{MnSb}_{11}$ is an underscreened Kondo lattice compound. A general characteristic of these compounds is that part of the entropy associated with the local magnetic moment (Mn spins) is removed by a transfer of part of the local d character to the conduction band.^{20,21} This transfer begins near the coherence temperature T^* and results in a large renormalization of the mass of quasiparticles at the Fermi energy and modification of the Fermi surface below T^* . Burch *et al.*¹² estimated that T^* is near the ferromagnetic transition temperature ($T^* \approx 50$ K). This is consistent with

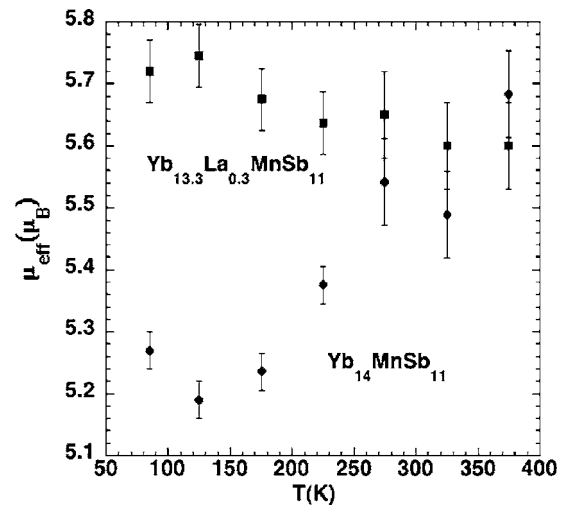


FIG. 6. Effective magnetic moment versus temperature extracted from dc susceptibility data taken in a field of 1 T. The Curie-Weiss temperature T_{CW} was fixed for each material and the data was fit to $\chi(\text{cm}^3/\text{mole Mn}) = \chi_0 + C/(T - T_{CW})$ over 50 K intervals, with $\mu_{eff} = (8C)^{1/2}$.

the present Hall data that indicate a jump in the carrier concentration (which is a measure of the topology of the Fermi surface) from about 1.2×10^{21} holes cm^{-3} above T_c to 1.9×10^{21} holes cm^{-3} well below T_c . Further studies of these materials are clearly needed, however, to substantiate the Kondo lattice interpretation of the present data. We also believe that further investigations of natural DMS, such as $\text{Yb}_{14}\text{MnSb}_{11}$, will provide additional insights into the complex physics of carrier mediated magnetism that will be essential to the understanding and design of actual spintronic devices.

It is a pleasure to acknowledge enlightening discussions with Kenneth Burch, David Singh, Victor Barzykin, Igor Zutic, Thomas Schulthess, and Steve Nagler. We were supported by the Oak Ridge National Laboratory, the UT-Battelle LLC, and the U.S. Department of Energy under Contract No. DE-AC05-00OR22725.

¹S. A. Wolf, D. D. Awschalom, R. A. Buhrman, J. M. Daughton, S. von Molnar, M. L. Roukes, A. Y. Chtchelkanova, and D. M. Treger, *Science* **294**, 1488 (2001).

²I. Zutic, J. Fabian, and Das Sarma, *Rev. Mod. Phys.* **76**, 323 (2004).

³A. H. MacDonald, P. Schiffer, and N. Samarth, *Nat. Mater.* **4**, 195 (2005), and references therein.

⁴T. Dietl and H. Ohno, *MRS Bull.* **28**, 714 (2003).

⁵J. Y. Chan, M. M. Olmstead, S. M. Kauzlarich, and D. J. Webb, *Chem. Mater.* **10**, 3583 (1998).

⁶S. M. Kauzlarich, in *Chemistry, Structure and Bonding of Zintl Phases and Ions*, edited by S. M. Kauzlarich (VCH, New York, 1996), p. 245.

⁷A. P. Holm, S. M. Kauzlarich, S. A. Morton, G. D. Waddill, W. E.

Pickett, and J. G. Tobin, *J. Am. Chem. Soc.* **124**, 9894 (2002).

⁸I. R. Fisher, T. A. Wiener, S. L. Budko, P. C. Canfield, J. Y. Chan, and S. M. Kauzlarich, *Phys. Rev. B* **59**, 13829 (1999).

⁹A. Rehr, T. Y. Kuromoto, S. M. Kauzlarich, J. Delcastillo, and D. J. Webb, *Chem. Mater.* **6**, 93 (1994).

¹⁰D. Sanchez-Portal, R. M. Martin, S. M. Kauzlarich, and W. E. Pickett, *Phys. Rev. B* **65**, 144414 (2002).

¹¹T. Dietl, F. Matsukura, and H. Ohno, *Phys. Rev. B* **66**, 33203 (2002).

¹²K. S. Burch, A. Schafgans, N. P. Butch, T. A. Sayles, M. B. Maple, B. C. Sales, D. Mandrus, and D. N. Basov, *Phys. Rev. Lett.* **95**, 46401 (2005).

¹³L. Berger and G. Bergmann, *The Hall Effect and Its Applications*, edited by C. L. Chien and C. R. Westgate (Plenum, New York,

- 1980), p. 55.
- ¹⁴T. Jungwirth, Q. Niu, and A. H. MacDonald, Phys. Rev. Lett. **88**, 207208 (2002).
- ¹⁵Y. Taguchi, Y. Oohara, H. Yoshizawa, N. Nagaosa, and Y. Tokura, Science **291**, 2573 (2001).
- ¹⁶W. L. Lee, S. Watauchi, V. L. Miller, R. J. Cava, and N. P. Ong, Science **303**, 1647 (2004).
- ¹⁷B. C. Sales (unpublished).
- ¹⁸P. Fazekas, *Electron Correlation and Magnetism*, Lecture Notes in Physics Vol. 5 (World Scientific, London, 1999), p. 650.
- ¹⁹S. K. Malik and D. T. Adroja, Phys. Rev. B **43**, 6295 (1991).
- ²⁰S. Nakatsuji, D. Pines, and Z. Fisk, Phys. Rev. Lett. **92**, 16401 (2004).
- ²¹N. J. Curro, B. L. Young, J. Schmalian, and D. Pines, Phys. Rev. B **70**, 235117 (2004).
- ²²A. Fert and P. M. Levy, Phys. Rev. B **36**, 1907 (1987).